



Changes in the Sarcoplasmic Proteome of Beef Muscles with Differential Color Stability during Postmortem Aging

Mahesh N. Nair¹, Shuting Li², Carol M. Beach³,
Gregg Rentfrow², and Surendranath P. Suman^{2*}

¹Department of Animal Sciences, Colorado State University, Fort Collins, CO 80523, USA

²Department of Animal and Food Sciences, University of Kentucky, Lexington, KY 40546, USA

³Proteomics Core Facility, University of Kentucky, Lexington, KY 40506, USA

*Corresponding author. Email: spsuma2@uky.edu (S. P. Suman)

Abstract: Beef color is a muscle-specific trait, and sarcoplasmic proteome influences muscle-specific variations in beef color stability. Postmortem aging influences the color and sarcoplasmic proteome of beef muscles. Nonetheless, muscle-specific changes in sarcoplasmic proteome of beef muscles with differential color stability during aging have not been characterized yet. Therefore, our objective was to examine the changes in the sarcoplasmic proteome of 3 differentially color stable muscles from beef hindquarters during postmortem aging. *Longissimus lumborum* (LL), *psaos major* (PM), and *semitendinosus* (ST) separated from 8 ($n = 8$) beef carcasses (24 h postmortem) were subjected to aging in vacuum packaging (2°C) for 0, 7, 14, and 21 d. On each aging day, steaks were fabricated, and allotted to refrigerated storage (2°C) under aerobic packaging. Samples for proteome analysis obtained during fabrication were frozen at -80°C . Instrumental color and metmyoglobin reducing activity were evaluated on d 0, 3, and 6 of storage. Sarcoplasmic proteome was analyzed, and differentially abundant proteins were identified using mass spectrometry. Color attributes and biochemical parameters were influenced by muscle source and aging ($P < 0.05$); LL and ST had greater ($P < 0.05$) surface redness than PM. Aging also influenced surface redness, with 7-d aged steaks demonstrating greatest values ($P < 0.05$). Proteome analysis identified 135 protein spots differentially abundant ($P < 0.05$) between the muscles and aging time points indicating muscle-specific changes during aging. The identified proteins included glycolytic enzymes, proteins associated with energy metabolism, antioxidant proteins, chaperones, and transport proteins. Overall, the glycolytic enzymes were more abundant ($P < 0.05$) in color-stable muscles and at aging times with greater color stability, indicating that these proteins could be used as potential biomarkers for beef color.

Keywords: color stability, meat color, muscle-specificity, proteomics, sarcoplasmic proteome

Meat and Muscle Biology 2:1–17 (2018)

doi:10.22175/mmb2017.07.0037

Submitted 10 Jul. 2017

Accepted 27 Nov. 2017

Introduction

Color of fresh beef critically influences the consumers' purchase decisions (Mancini and Hunt,

2005; Suman et al., 2014). Discoloration adversely affects the consumer perception of meat quality, leading to product rejection and economic loss. The annual revenue loss for the US beef industry corresponding to surface discoloration has been estimated to be more than \$1 billion (Smith et al., 2000). Fresh meat color is primarily determined by the concentration of myoglobin and the equilibrium of the heme protein's redox forms. The redox state of myoglobin is highly influenced by its interaction with cellular organelles and biomolecules in the postmortem skeletal muscles (Faustman et al., 2010; Suman and Joseph, 2013; Suman and Nair, 2017).

This project was supported by the Agriculture and Food Research Initiative Grant 2012-67018-30166 from the USDA National Institute of Food and Agriculture. Mass spectrometric analysis was performed at the University of Kentucky's Proteomics Core Facility, supported in part by funds from the Office of the Vice President for Research. This is publication number 17-07-056 of the Kentucky Agricultural Experiment Station and is published with the approval of the director.

Several intrinsic (sex, endogenous antioxidants, animal age, muscle source, and pH) and extrinsic (post-mortem aging, temperature, light, and packaging) factors influence beef color stability (Neethling et al., 2017; Suman et al., 2014; Mancini and Hunt, 2005). Among these factors, muscle source received significant attention (McKenna et al., 2005; Von Seggern et al., 2005). Muscles in a beef carcass vary in their physicochemical and biochemical characteristics due to specific anatomical locations, physiological functions, energy metabolism, and fiber type (Hunt and Hedrick, 1977). McKenna et al. (2005) categorized beef muscles into high, moderate, low, and very low color stability based on the objective measures of discoloration.

Postmortem aging (in vacuum packaging) is a common meat industry practice to improve tenderness and palatability, and beef subprimals are aged/stored for an average of 20 d in retail establishments (Guelker et al., 2013). The cellular and biochemical mechanisms that govern the meat quality attributes undergo changes during postmortem aging. As aging time increases, there is decreased competition from mitochondria for oxygen, thereby improving myoglobin oxygenation, resulting in improved blooming (Mac Dougall, 1982; Mancini and Ramanathan, 2014). However, Lee et al. (2008) reported that aging beyond 14 d adversely affects color in beef gluteus medius. Aging can also influence cellular mechanisms (such as reducing enzymes, oxygen scavenging enzymes, and mitochondria) responsible for meat color stability, resulting in lower color stability during subsequent retail display (King et al., 2012; English et al., 2016).

Sarcoplasmic proteins play a critical role in fresh meat color due to their ability to interact directly with myoglobin (Renerre et al., 1996), and the role of sarcoplasmic proteome on muscle-specific beef color stability has been reported previously. Joseph et al. (2012) compared the sarcoplasmic proteome of color-stable *longissimus lumborum* (LL) and color-labile *psaos major* (PM), and reported differential abundance of several proteins, including metabolic enzymes, antioxidant proteins, and chaperones. Further, Wu et al. (2015, 2016) reported differentially abundant sarcoplasmic proteins in LL, PM, and *semitendinosus* (ST) muscle from Luxi yellow cattle during postmortem storage for 0, 5, 10, and 15 d. Postmortem aging also influences the sarcoplasmic proteome, and aging alters meat quality traits (color, pH, and water holding capacity) in beef LL by affecting the sarcoplasmic protein patterns (Marino et al., 2014). Together these studies indicated that muscle source and aging can affect sarcoplasmic proteome profile, which in turn can influence meat

color. Nonetheless, the muscle-specific changes in sarcoplasmic proteome during aging of beef muscles have not been examined yet. Therefore, the objective of the current study was to examine the changes in sarcoplasmic proteome of 3 differentially color stable muscles (LL, PM, and ST) from beef hindquarters during aging.

Materials and Methods

Beef fabrication

The LL, PM, and ST muscles were excised (24 h postmortem) from both sides of eight ($n = 8$) beef carcasses (USDA Choice; A maturity) obtained from the USDA-inspected meat laboratory of the University of Kentucky. Each muscle was divided into two-equal length sections, resulting in 4 muscle sections per carcass. The muscle sections were vacuum packaged (99% vacuum; Sipromac Model 600A, Drummondville, Quebec, Canada) in Prime Source vacuum pouches (3 mil, Bunzl Koch Supplies Inc., Kansas City, MO), and randomly assigned to aging at 2°C for either 0, 7, 14, or 21 d. After aging, muscle sections were fabricated into 1.92-cm thick steaks. Abbreviations were used to indicate muscles aged for 0-d (LL0, PM0, and ST0), 7-d (LL7, PM7, and ST7), 14-d (LL14, PM14, and ST14), and 21-d (LL21, PM21, and ST21). Samples for proteome analysis (approximately 50 g) were collected during fabrication, immediately vacuum-packaged, and frozen at -80°C. Six steaks were individually placed on Styrofoam trays, aerobically overwrapped with oxygen-permeable polyvinyl chloride film (15,500 – 16,275 cm³/m²/24 h oxygen transmission rate at 23°C), and were assigned randomly for 0, 3, and 6 d of refrigerated storage (2°C) in dark (Mancini et al., 2009). On each storage day, 2 steaks were utilized for evaluation of instrumental color parameters and metmyoglobin reducing activity (MRA).

Instrumental color

On d 0 of storage, the instrumental color attributes were evaluated after allowing the steaks to bloom for 2 h at 2°C after fabrication, whereas on the remaining storage days (3 and 6) the measurements were taken on the oxygen-exposed steak surfaces. A HunterLab LabScan XE colorimeter (Hunter Associates Laboratory, Reston, VA) with 2.54-cm diameter aperture, illuminant A, and 10° standard observer was used to measure CIE lightness (L^*) and redness (a^*) values from 3 random locations (American Meat Science Association, 2012). The colorimeter was calibrated with standard black

and white plates. Surface color stability was estimated using the ratio of reflectance at 630 nm and 580 nm (R630/580) obtained from the colorimeter readings.

Metmyoglobin reducing activity (MRA)

The methodology described by Sammel et al. (2002) was used for evaluating MRA. Samples from the oxygen-exposed surface (approximately $2.5 \times 2.5 \times 2.5$ cm cubes with no visible fat or connective tissue) were submerged in 0.3% solution of sodium nitrite (Sigma-Aldrich Co., St. Louis, MO) for 20 min at room temperature to facilitate metmyoglobin formation. The samples were removed from the solution after 20 min, blotted dry to remove the surface nitrate solution, and then vacuum packaged. The reflectance spectra from 700 to 400 nm were recorded immediately after vacuum packaging on the light-exposed surface using a HunterLab LabScan XE colorimeter, and was used to calculate pre-incubation surface metmyoglobin values (American Meat Science Association, 2012). Each of the vacuum-packaged samples were then incubated at 30°C for 2 h to induce reduction of metmyoglobin. After incubation, the reflectance data were collected again and were used to calculate post-incubation metmyoglobin values (American Meat Science Association, 2012). The MRA was calculated using the equation: $MRA = 100 \times [(\% \text{ pre-incubation surface metmyoglobin} - \% \text{ post-incubation surface metmyoglobin}) / \% \text{ pre-incubation surface metmyoglobin}]$.

Isolation of sarcoplasmic proteome

The LL, PM, and ST samples ($n = 8$) frozen (-80°C) on each of the aging days (0, 7, 14, and 21) were used for sarcoplasmic proteome isolation. Frozen muscle tissue (5 g) devoid of any visible fat and connective tissue was homogenized in 25 mL ice-cold extraction buffer (40 mM Tris, 5 mM EDTA, pH 8.0) using a Waring blender (Waring Commercial, Torrington, CT). The homogenate was then centrifuged at $10,000 \times g$ for 15 min at 4°C . The supernatant consisting of the sarcoplasmic proteome extract was filtered (Whatman No. 1 filter paper) and utilized for subsequent analysis (Joseph et al., 2012).

Two-dimensional electrophoresis (2-DE)

The protein concentration of the sarcoplasmic proteome extract from each sample was determined in duplicate employing Bradford assay (Bradford, 1976) using the Bio-Rad Protein Assay kit (Bio-Rad Laboratories Inc., Hercules, CA). The sarcoplasmic proteome (900 μg) was mixed with rehydration buffer

(Bio-Rad Laboratories Inc.) optimized to 7 M urea, 2 M thiourea, 20 mM DTT, 4% CHAPS, 0.5% Bio-Lyte 5/8 ampholyte, and 0.001% Bromophenol blue. The mixture of sarcoplasmic proteome and rehydration buffer was loaded onto immobilized pH gradient (IPG) strips (pH 5 to 8, 17 cm; Bio-Rad Laboratories Inc.) and was subjected to passive rehydration for 16 h (Joseph et al., 2012). Protean IEF Cell system (Bio-Rad Laboratories Inc.) was used for the first dimension isoelectric focusing, which enables the separation of proteins based on their isoelectric point (pI). A low voltage (50 V) was applied during the initial active rehydration for 4 h, followed by a linear increase in voltage, and a final rapid voltage ramping to attain a total of 60 kVh.

After isoelectric focusing, the IPG strips were equilibrated with equilibration buffer I (6 M urea, 0.375 M Tris-HCl, pH 8.8, 2% SDS, 20% glycerol, 2% (w/v) DTT; Bio-Rad) followed by equilibration buffer II (6 M urea, 0.375 M Tris-HCl, pH 8.8, 2% SDS, 20% glycerol, 2.5% (w/v) iodoacetamide; Bio-Rad Laboratories Inc.) for 15 min each. Separation of proteins in the second dimension based on molecular weight was performed using 13.5% sodium dodecyl sulfate polyacrylamide gel electrophoresis (SDS PAGE; 38.5:1 ratio of acrylamide to bis-acrylamide) by loading the equilibrated strips on to SDS gel with an agarose overlay in a Protean II Multicell system (Bio-Rad Laboratories Inc.) using running buffer (25 mM Tris, 192 mM Glycine, 0.1% SDS). A constant voltage of 100 V was applied for approximately 16 h for the separation of proteins in the second dimension. Gels staining was performed using Colloidal Coomassie Blue for 48 h followed by destaining for 48 h or until sufficient background clearing was obtained. Each muscle (LL, PM, or ST) during the aging days (0, 7, 14, or 21) from all the carcasses ($n = 8$) was analyzed in duplicate resulting in a total of 192 gels.

Gel image analysis

The gel images were obtained using VersaDoc imager (Bio-Rad Laboratories Inc.) and were analyzed using PDQUEST software (Bio-Rad Laboratories Inc.). Comparisons were made for muscle-specificity on each day of aging and also for changes to each muscle during aging (0-d aging sample for each muscle was considered as control). All gel images were processed and analyzed under similar parameters. Protein spots identified during spot detection were automatically matched with the spots of a master gel used as a reference. Further, landmark spots were used to confirm spot matching across all gels and manual verification was used to screen out

artifacts or incorrectly identified spots. Relative volume of each spot in a gel was normalized as a percentage of the total volume of all spots detected on the gel. A protein spot was considered to be differentially abundant when it demonstrated 1.5-fold intensity difference between the treatments and was associated with $P < 0.05$ in a pairwise Student's t test.

Liquid chromatography-electrospray ionization-tandem mass spectrometry (LC-ESI-MS/MS) analysis

For confirmation of protein identity, duplicate spots from the corresponding gels were subjected to mass spectrometric protein identification. The protein spots differentially abundant between the treatments were excised from the gel and then subjected to dithiothreitol reduction, iodoacetamide alkylation, and in-gel trypsin digestion. The peptides formed were extracted, concentrated and injected for nano-LC-MS/MS analysis using an LTQ-Orbitrap mass spectrometer (Thermo Fisher Scientific Inc., Waltham, MA) coupled with an Eksigent Nanoflex cHiPLC system (Eksigent Technologies, Dublin, CA) through a nano electrospray ionization source. A reverse phase cHiPLC column (75 $\mu\text{m} \times 150 \text{ mm}$) operated at a flow rate of 300 nL/min was used for separation of the peptides. Mobile phase A consisted of water with 0.1% (v/v) formic acid, and mobile phase B contained acetonitrile with 0.1% (v/v) formic acid. A 50 min gradient was applied: initial 3% mobile phase B was increased linearly to 50% in 24 min and further to 85% and 95% for 5 min each before it was decreased to 3%, and the column was re-equilibrated. The mass analysis method consisted eight scan events per segment. The first scan event was an Orbitrap MS scan (100 to 1,600 m/z) with 60,000 resolutions for parent ions which was followed by data dependent MS/MS for fragmentation of the 7 most intense ions through collision induced dissociation.

MS/MS protein identification

The LC-MS/MS data were submitted to a local Mascot server for MS/MS protein identification via Proteome Discoverer (version 1.3, Thermo Fisher Scientific Inc., Waltham, MA) against a *Bos taurus* database from National Center for Biotechnology Information. Parameters used in the MASCOT MS/MS ion search were: trypsin digest with a maximum of 2 miscleavages, cysteine carbamidomethylation, methionine oxidation, a maximum of 0.001% MS error tolerance, and a maximum of 0.8 Da MS/MS error tolerance. A decoy database was built and searched. Filter

settings that determine false discovery rates (FDR) are used to distribute the confidence indicators for the peptide matches. Peptide matches that passed the filter associated with the strict FDR (target setting of 0.01) were assigned as high confidence. For the MS/MS ion search, proteins with 2 or more high confidence peptides were considered unambiguous identifications without manual inspection. Proteins identified with one high confidence peptide were manually inspected and confirmed.

Statistical analysis

The LL, PM, and ST muscles from 8 beef carcasses ($n = 8$) were utilized for this study. The experimental design was a split-split plot with muscle source (LL, PM, and ST) as whole plot and aging time (0, 7, 14, and 21 d) as subplot. For color characteristics, display day (0, 3, and 6) was set as a sub-sub plot. Carcass was considered as random effect. The data were analyzed using PROC MIXED procedure of SAS Version 9.4 (SAS Institute Inc., Cary, NC), and the differences among means were detected using the least significant difference (LSD) at 5% level.

Results and Discussion

Instrumental color and biochemical attributes

There was no aging \times muscle \times storage interaction ($P = 0.4422$; Table 1) for lightness (L^* value). Muscle-specificity ($P < 0.0001$) was observed for lightness, with ST having greatest ($P = 0.0013$) lightness, whereas LL and PM exhibited similar lightness ($P = 0.2399$). In agreement, muscle-specificity in lightness has been reported previously in beef (McKenna et al., 2005; Joseph et al., 2012, Canto et al., 2016). Overall, aging resulted in an increase ($P < 0.0001$) in lightness of the muscles in the present study. In partial agreement, Marino et al. (2014) reported that aging for 21 d resulted in an increase in lightness of beef *longissimus dorsi*. However, in the present study, 7-d aged steaks had similar ($P > 0.05$) lightness as 14-d and 21-d aged steaks; thus, aging beyond 7 d did not increase the lightness. In contrast, English et al. (2016) reported that L^* values increased in beef LL aged for 62 d compared to the LL counterparts aged for 21 d.

Surface redness (a^* value) of LL, PM, and ST during storage after aging for 0, 7, 14, and 21 d is presented in Table 2. There was no aging \times muscle \times storage interaction ($P = 0.5440$). However, aging, muscle source, and storage days influenced surface redness

Table 1. Effect of aging¹ and muscle source² on surface lightness (L^* value) of beef steaks ($n = 8$) during refrigerated storage (2°C) for 6 d under aerobic packaging (SEM = 1.0384)

Aging (A)	Muscle (M)	Storage days (S)			P -values
		0	3	6	
0 d	LL	41.15	43.02	43.69	A < 0.0001
	PM	45.11	44.17	44.54	M 0.0003
	ST	44.43	45.33	46.06	S 0.0578
7 d	LL	44.29	45.42	45.80	A × M 0.3153
	PM	45.61	44.83	43.92	A × S < 0.0001
	ST	47.49	47.91	47.86	M × S 0.0010
14 d	LL	45.90	45.79	43.54	A × M × S 0.4422
	PM	47.00	44.70	44.92	
	ST	48.82	48.63	47.42	
21 d	LL	44.48	45.13	43.90	
	PM	45.84	45.26	44.41	
	ST	48.04	48.15	46.91	

¹Aging in vacuum packaging at 2°C.²LL, *Longissimus lumborum*; PM, *Psoas major*; ST, *Semitendinosus*.

($P < 0.0001$). Redness was influenced by aging, with greatest ($P < 0.0001$) redness observed for the 7-d aged steaks. However, there was no difference in redness between 14-d and 21-d aged steaks ($P = 0.6605$). Among the muscles, LL had greater redness than PM ($P < 0.0001$), whereas it had similar redness to ST ($P = 0.1625$); ST also demonstrated greater ($P = 0.0002$) redness than PM. In agreement, McKenna et al. (2005) observed no difference in redness of LL and ST dur-

ing retail display, whereas PM demonstrated a lower redness than LL and ST. On the other hand, Seyfert et al. (2006) reported that the color stability of these muscles during retail display followed the order: LL (most stable) > ST > PM (least stable). Aging × storage ($P < 0.0001$) and muscle × storage ($P < 0.0001$) interactions were observed for a^* value. Aged steaks (7, 14, or 21 d) had greater ($P < 0.0001$) initial redness (on d 0 of storage) compared to steaks that were not aged.

Ratio of reflectance at 630 nm and 580 nm (R630/580) is used as an indirect estimate of meat surface color stability. A greater ratio indicates greater color stability and lower metmyoglobin content. There was no aging × muscle × storage interaction ($P = 0.8799$; Table 3) for R630/580. However, aging, muscle source, and storage days influenced the surface color stability ($P < 0.0001$). The muscles followed the order LL > ST > PM for the color stability, in agreement with categorization of these muscles as color-stable, intermediately color-stable, and color-labile, respectively (McKenna et al., 2005, Joseph et al., 2012). Aging also influenced ($P < 0.0001$) the surface color stability, with 7-d aged steaks having the highest ($P < 0.05$) R630/580 value, whereas 0-d aged, 14-d aged, and 21-d aged steaks demonstrated similar ($P > 0.05$) surface color stability.

The MRA indicates the ability of meat to reduce ferric metmyoglobin to ferrous redox forms (deoxy- or oxymyoglobin). A higher value indicates that the muscle has a greater inherent ability to reduce metmyoglobin, thereby improving the meat color stability. There was an

Table 2. Effect of aging¹ and muscle source² on surface redness (a^* value) of beef steaks ($n = 8$) during refrigerated storage (2°C) for 6 d under aerobic packaging (SEM = 0.93)

Aging (A)	Muscle (M)	Storage days (S)			P -values
		0	3	6	
0 d	LL	28.04	28.32	26.84	A < 0.0001
	PM	30.63	22.85	19.05	M < 0.0001
	ST	29.04	26.74	23.92	S < 0.0001
7 d	LL	31.29	30.89	28.08	A × M 0.5312
	PM	31.68	23.58	20.12	A × S < 0.0001
	ST	31.46	29.61	25.85	M × S < 0.0001
14 d	LL	31.67	29.02	25.17	A × M × S 0.5440
	PM	31.40	22.66	18.00	
	ST	31.88	28.46	23.59	
21 d	LL	30.94	28.98	25.27	
	PM	31.56	22.52	19.12	
	ST	31.48	28.68	21.88	

¹Aging in vacuum packaging at 2°C.²LL, *Longissimus lumborum*; PM, *Psoas major*; ST, *Semitendinosus*.**Table 3.** Effect of aging¹ and muscle source² on surface color stability (R630/580) of beef steaks ($n = 8$) during refrigerated storage (2°C) for 6 d under aerobic packaging (SEM = 0.2441)

Aging (A)	Muscle (M)	Storage days (S)			P -values
		0	3	6	
0 d	LL	5.07	4.28	3.61	A 0.0003
	PM	5.09	2.70	2.17	M < 0.0001
	ST	4.72	3.58	3.01	S < 0.0001
7 d	LL	5.57	4.85	3.96	A × M 0.5415
	PM	5.31	2.80	2.23	A × S 0.7451
	ST	5.42	4.26	3.35	M × S < 0.0001
14 d	LL	5.36	4.23	3.33	A × M × S 0.8799
	PM	4.96	2.72	2.08	
	ST	4.93	3.90	2.92	
21 d	LL	5.28	4.31	3.41	
	PM	5.11	2.69	2.27	
	ST	4.95	3.99	2.69	

¹Aging in vacuum packaging at 2°C.²LL, *Longissimus lumborum*; PM, *Psoas major*; ST, *Semitendinosus*.

aging \times muscle \times storage interaction ($P = 0.0351$; Table 4) for MRA. However, MRA was not altered by aging for 21 d ($P = 0.0973$). In contrast, previous research indicated that extended aging (for 42 or 62 d) decreased MRA probably due to the depletion of reducing enzymes and mitochondrial substrates (English et al., 2016). The observed differences in MRA between our study and the previous research could be attributed to the difference in the aging days (21 vs. 42 or 62).

The MRA was muscle-specific, with PM having the lowest ($P < 0.0001$) value, whereas LL and ST had similar ($P = 0.0793$) values. Previous research (Joseph et al., 2012; Canto et al., 2016) also indicated greater MRA for LL steaks compared to PM ones. The MRA results are also in agreement with the surface redness (a^* value) and color stability (R630/580) data. An interesting observation in the current study was the increase ($P < 0.05$) in MRA of PM on d 6 of storage compared to d 3 of storage in 7-d, 14-d, and 21-d aged steaks (Table 4). However, this pattern was not observed in LL and ST. The observed variations in MRA during later stages of storage could be a muscle-specific change happening in PM steaks. One possible hypothesis to explain this observation is that the combination of prolonged aging and storage in an already color-labile muscle (PM) could have led to degradation of mitochondria towards the end of storage, releasing more mitochondrial enzymes, which could potentially improve MRA, without a concomitant increase in the surface redness. Nonetheless, we did not evaluate mitochondrial deg-

radation to confirm this hypothesis. In partial support, muscle-specificity in beef mitochondrial functionality has been reported previously, with mitochondria from PM having lower mitochondrial MRA and oxygen consumption rate after storage for 7 d compared to mitochondria from *longissimus dorsi* (Belskie et al., 2015).

Sarcoplasmic proteome analyses

The summary of differentially abundant sarcoplasmic protein spots identified by image analysis is presented in Table 5. The representative gel images of sarcoplasmic proteome of LL during aging are presented in Fig. 1. Eighty-six protein spots were detected to be differentially abundant between LL, PM, and ST indicating muscle-specific changes during aging. Aging-related changes in the proteome of each muscle were examined using 0-d aged sample from each muscle as control. A total of 49 protein spots were identified to be differentially abundant with aging (14 protein spots in LL, 17 protein spots in PM, and 18 protein spots in ST). These results indicated that the changes occurring in sarcoplasmic proteome of beef hindquarter muscles (LL, PM, and ST) are muscle- and aging-specific in nature (Tables 6 to 12). Multiple protein spots were identified as the same protein in mass spectrometric analyses. These protein spots had similar molecular weights, but different isoelectric points, which could be attributed to the existence of different isoforms and possible post-translational modifications such as phosphorylation (Canto et al.,

Table 4. Effect of aging¹ and muscle source² on metmyoglobin reducing activity (MRA) of beef steaks ($n = 8$) during refrigerated storage (2°C) for 6 d under aerobic packaging (SEM = 5.65)

Aging (A)	Muscle (M)	Storage days (S)			<i>P</i> -values	
		0	3	6		
0 d	LL	63.81	47.36	46.61	A	0.0973
	PM	34.93	14.63	10.24	M	< 0.0001
	ST	66.30	42.54	41.63	S	< 0.0001
7 d	LL	56.22	48.61	41.60	A \times M	0.1622
	PM	20.24	6.24	18.28	A \times S	0.1592
	ST	55.20	56.62	35.39	M \times S	0.0010
14 d	LL	56.99	37.19	38.39	A \times M \times S	0.0351
	PM	22.78	7.91	23.92		
	ST	47.02	41.63	39.08		
21 d	LL	56.70	42.80	21.12		
	PM	20.32	11.20	30.31		
	ST	59.33	42.90	42.49		

¹Aging in vacuum packaging at 2°C.

²LL, *Longissimus lumborum*; PM, *Psoas major*; ST, *Semitendinosus*.

Table 5. Summary of differentially abundant protein spots in the sarcoplasmic proteome of beef *longissimus lumborum* (LL), *psoas major* (PM), and *semitendinosus* (ST; $n = 8$) aged for 0, 7, 14, and 21 d

Muscle-specificity		Aging	
Treatment	Number of protein spots	Treatment	Number of protein spots
LL0 vs. PM0	4 spots	LL0 vs. LL7	2 spots
LL0 vs. ST0	4 spots	LL0 vs. LL14	7 spots
PM0 vs. ST0	7 spots	LL0 vs. LL21	5 spots
LL7 vs. PM7	11 spots	PM0 vs. PM7	8 spots
LL7 vs. ST7	3 spots	PM0 vs. PM14	6 spots
PM7 vs. ST7	14 spots	PM0 vs. PM21	3 spots
LL14 vs. PM14	14 spots	ST0 vs. ST7	10 spots
LL14 vs. ST14	6 spots	ST0 vs. ST14	5 spots
PM14 vs. ST14	6 spots	ST0 vs. ST21	3 spots
LL21 vs. PM21	5 spots	Total	49 spots
LL21 vs. ST21	2 spots		
PM21 vs. ST21	10 spots		
Total	86 spots		

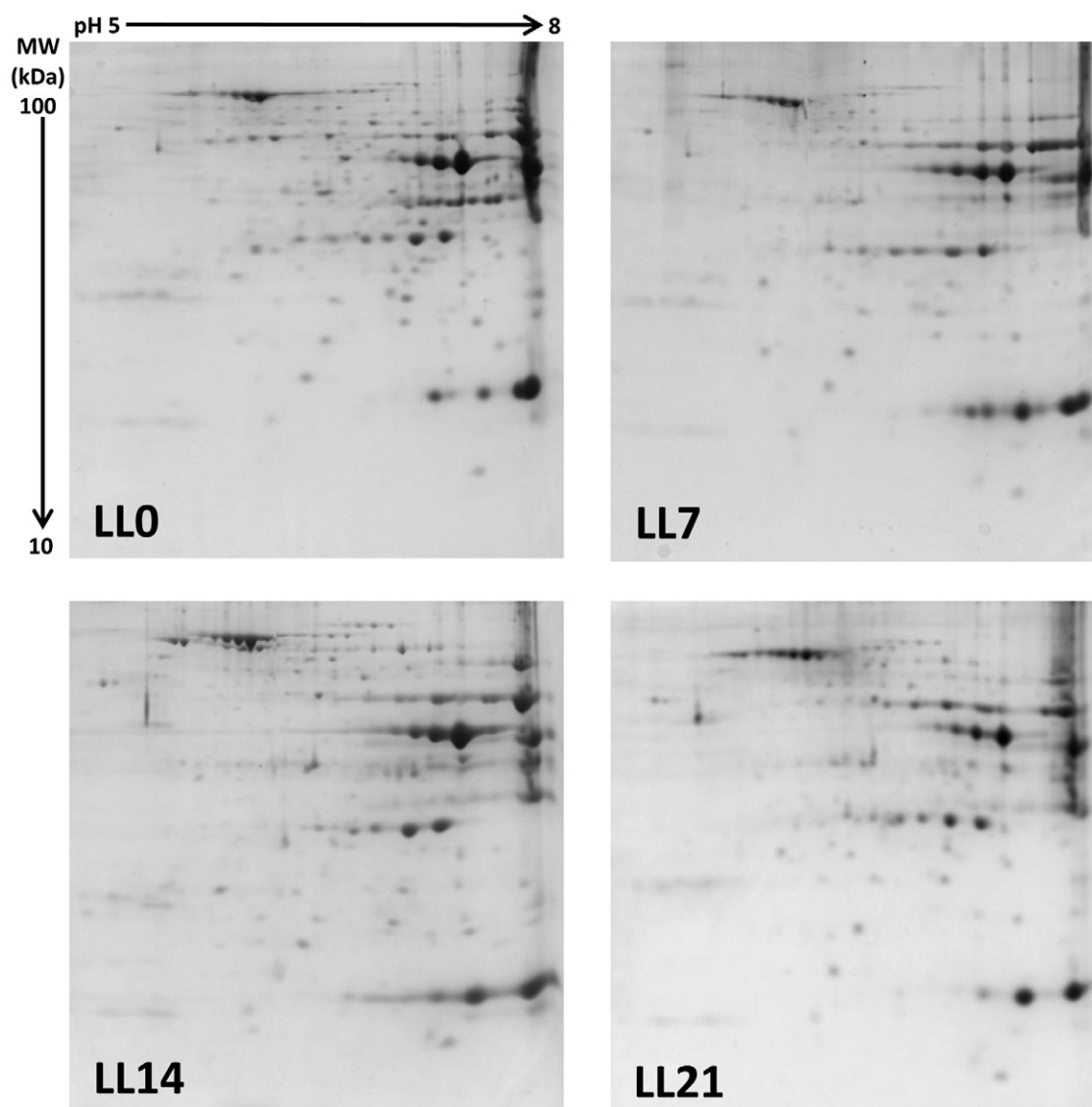


Figure 1. Representative 2-dimensional gel electrophoresis maps of sarcoplasmic proteome extracted from beef *longissimus lumborum* (LL) after 0 (LL0), 7 (LL7), 14 (LL14) and 21 (LL21) days of aging separated using an immobilized pH gradient (IPG) 5 to 8 strip in the first dimension and 13.5% SDS gel in the second dimension.

2015; Anderson et al., 2014). Phosphorylation can shift the isoelectric point of the proteins with minimal or no change in molecular weight, and could be indicative of the functional status of the proteins.

Previous proteomic investigations have also reported differential abundance of sarcoplasmic proteins between muscles in the beef carcass. Joseph et al. (2012) compared the sarcoplasmic proteome profile of beef LL and PM, and attributed the greater color stability of LL to the greater abundance of metabolic enzymes, antioxidant proteins, and chaperones compared to color-labile PM. Similarly, Wu et al. (2016) reported several glycolytic and antioxidant proteins to be differentially abundant in LL and PM during post-mortem storage (15 d) in Chinese Luxi yellow cattle.

Clerens et al. (2016) performed proteomic and peptidomic analysis of 4 muscles (LL, PM, ST, and infraspinatus) from New Zealand-raised Angus steers and reported significant intensity differences between many proteins, including hemoglobin subunit β , carbonic anhydrase 3, triosephosphate isomerase, phosphoglycerate mutase 2, serum albumin and β enolase. Marino et al. (2014) demonstrated that aging for 21 d influenced the sarcoplasmic proteome profile of beef LL in Romagnola \times Podolian, Podolian, and Friesian cattle, with the abundance of proteins such as β -enolase, creatine kinase M-type, fructose-bisphosphate aldolase B, glyceraldehyde 3-phosphate dehydrogenase, triosephosphate isomerase, glutathione S-transferase P, and protein DJ-1 decreasing during aging.

Table 6. Differentially abundant sarcoplasmic proteins in beef *longissimus lumborum* (LL), *psoas major* (PM), and *semitendinosus* (ST) steaks ($n = 8$) on d 0 of aging

Protein	Accession number	Score/matched peptides	Sequence coverage, %	Over-abundant	Spot ratio	Function
LL0 vs. PM0						
Serum albumin	P02769	10550.37/87	90.77	LL0	1.74 ^a	Transport
Creatine kinase M-type	Q9XSC6	4573.87/53	81.10	LL0	1.80 ^a	Energy metabolism
Creatine kinase M-type	Q9XSC6	10790.77/62	83.99	LL0	1.84 ^a	Energy metabolism
Myoglobin	P02192	2665.01/24	99.35	PM0	0.60 ^a	Oxygen transport
LL0 vs. ST0						
Phosphoglucomutase-1	Q08DP0	3544.00/56	69.22	LL0	1.53 ^b	Glycolytic enzyme
Serotransferrin	Q29443	4772.99/84	85.09	LL0	1.53 ^b	Transport protein
Glyceraldehyde-3-phosphate dehydrogenase	P10096	2812.92/30	80.48	LL0	3.33 ^b	Glycolytic enzyme
Beta-enolase	Q3ZC09	4499.71/53	79.95	LL0	3.23 ^b	Glycolytic enzyme
PM0 vs. ST0						
Serotransferrin	Q29443	6542.32/78	81.82	PM0	1.67 ^c	Transport protein
Creatine kinase M-type	Q9XSC6	2777.04/48	72.18	ST0	0.51 ^c	Energy metabolism
Creatine kinase M-type	Q9XSC6	6090.00/53	81.63	ST0	0.45 ^c	Energy metabolism
Glyceraldehyde-3-phosphate dehydrogenase	P10096	4260.65/35	71.77	PM0	1.93 ^c	Glycolytic enzyme
Myoglobin	P02192	3878.67/26	93.51	PM0	1.68 ^c	Oxygen transport
Superoxide dismutase [Mn], mitochondrial	P41976	269.87/11	29.73	PM0	1.83 ^c	Antioxidant
L-lactate dehydrogenase A	P19858	1346.58/34	85.24	PM0	6.88 ^c	Energy metabolism

^aSpot ratio of LL0/PM0.^bSpot ratio of LL0/ST0.^cSpot ratio of PM0/ST0.

Functional roles of differentially abundant proteins

The proteins that are differentially abundant between the muscles during aging could be categorized mainly as: (1) glycolytic enzymes, (2) proteins related to energy metabolism, (3) antioxidant proteins, (4) chaperones, and (5) transport proteins.

Glycolytic enzymes

The glycolytic enzymes that were differentially abundant between the treatment groups included triosephosphate isomerase, glyceraldehyde-3-phosphate dehydrogenase, enolase (α and β), and phosphoglucomutase-1. In general, the glycolytic enzymes were more abundant ($P < 0.05$) in LL and ST compared to PM. The greater abundance of glycolytic enzymes in these muscles could be a reflection of the inherent differences in their muscle fiber types. The LL and ST are considered glycolytic muscles, whereas PM is considered an oxidative muscle (Hunt and Hedrick, 1977; Kirchofer et al., 2002). However, we also observed differential abundance of glycolytic enzymes within the same muscle during aging. The LL0 had lower abundance ($P < 0.05$) of glycolytic enzymes (enolase, phosphoglucomutase-1) compared to LL14 and LL21, except that of glyceraldehyde-3-phosphate dehydroge-

nase which was of greater abundance ($P < 0.05$) in LL0 (Table 10). However, aging did not demonstrate any specific trend in PM and ST on the differentially abundant glycolytic proteins (Tables 11 and 12).

Among the glycolytic enzymes, triosephosphate isomerase catalyzes the interconversion of glyceraldehyde 3-phosphate and dihydroxyacetone phosphate (Albery and Knowles, 1976). Further, glyceraldehyde-3-phosphate dehydrogenase catalyzes the reversible conversion of glyceraldehyde-3-phosphate and NAD^+ to 1,3-bisphosphoglycerate and NADH (Kim and Dang, 2005). Enolase, expressed as 2 isozymes (α and β), is involved in the conversion of 2-phosphoglycerate to phosphoenolpyruvate, the ninth and penultimate step of glycolysis (Hoorn et al., 1974). Alpha enolase is ubiquitously expressed in tissues, whereas β -enolase is found most abundantly in skeletal muscle tissue. Phosphoglucomutase-1 is involved in generating glucose-6-phosphate from glycogen stores to be used for glycolysis and energy production (Cori et al., 1938). Although, phosphoglucomutase is not an enzyme in 1 of the 10 steps of glycolysis, we categorized this protein with glycolytic enzymes because glucose-6-phosphate (the common end product of glycogenolysis happening during the postmortem period) is a metabolite of the glycolytic pathway which can be converted to fructose-

Table 7. Differentially abundant sarcoplasmic proteins in beef *longissimus lumborum* (LL), *psaos major* (PM), and *semitendinosus* (ST) steaks ($n = 8$) on d 7 of aging

Protein	Accession number	Score/matched peptides	Sequence coverage, %	Over-abundant	Spot ratio	Function
LL7 vs. PM7						
Heat shock cognate protein (71 kDa)	P19120	2591.04/48	68.46	LL7	3.90 ^a	Chaperone
Serum albumin	P02769	5343.08/65	85.01	LL7	2.27 ^a	Transport
Serum albumin	P02769	10468.95/78	88.14	LL7	2.90 ^a	Transport
Triosephosphate isomerase	Q5E956	5553.64/27	93.98	LL7	2.00 ^a	Glycolytic enzyme
Triosephosphate isomerase	Q5E956	5345.41/23	91.57	LL7	1.59 ^a	Glycolytic enzyme
Creatine kinase M-type	Q9XSC6	3331.35/34	70.60	LL7	2.19 ^a	Energy metabolism
Creatine kinase M-type	Q9XSC6	4966.46/44	76.12	LL7	3.93 ^a	Energy metabolism
Triosephosphate isomerase	Q5E956	6505.02/29	93.98	LL7	1.53 ^a	Glycolytic enzyme
Creatine kinase M-type	Q9XSC6	8811.88/50	80.31	LL7	6.46 ^a	Energy metabolism
Myoglobin	P02192	3921.09/23	93.51	PM7	0.54 ^a	Oxygen transport
Beta-enolase	Q3ZC09	8605.29/50	72.81	LL7	4.65 ^a	Glycolytic enzyme
LL7 vs. ST7						
Heat shock cognate protein (71 kDa)	P19120	2516.15/50	66.00	LL7	2.75 ^b	Chaperone
Serum albumin	P02769	6468.62/75	85.50	LL7	1.55 ^b	Transport
Serum albumin	P02769	8481.16/69	84.84	LL7	1.63 ^b	Transport
PM7 vs. ST7						
Superoxide dismutase [Cu-Zn]	P00442	880.28/11	90.79	PM7	1.65 ^c	Antioxidant
Triosephosphate isomerase	Q5E956	1267.16/22	91.57	ST7	0.66 ^c	Glycolytic enzyme
Triosephosphate isomerase	Q5E956	4511.84/29	93.98	ST7	0.61 ^c	Glycolytic enzyme
Triosephosphate isomerase	Q5E956	4038.72/29	93.98	ST7	0.45 ^c	Glycolytic enzyme
Triosephosphate isomerase	Q5E956	4518.14/27	93.98	ST7	0.59 ^c	Glycolytic enzyme
Creatine kinase M-type	Q9XSC6	866.26/29	60.37	ST7	0.33 ^c	Energy metabolism
Triosephosphate isomerase	Q5E956	7573.39/26	93.98	ST7	0.66 ^c	Glycolytic enzyme
Creatine kinase M-type	Q9XSC6	2096.38/39	75.07	ST7	0.31 ^c	Energy metabolism
Creatine kinase M-type	Q9XSC6	3517.53/45	76.38	ST7	0.16 ^c	Energy metabolism
Myoglobin	P02192	2733.71/19	91.56	PM7	3.32 ^c	Oxygen transport
Triosephosphate isomerase	Q5E956	6566.88/30	93.98	ST7	0.53 ^c	Glycolytic enzyme
Myoglobin	P02192	3690.03/19	91.56	PM7	2.03 ^c	Oxygen transport
Creatine kinase M-type	Q9XSC6	10653.78/57	94.23	ST7	0.28 ^c	Energy metabolism
Beta-enolase	Q3ZC09	4322.40/46	76.04	ST7	0.38 ^c	Glycolytic enzyme

^aSpot ratio of LL7/PM7.^bSpot ratio of LL7/ST7.^cSpot ratio of PM7/ST7.

6-phosphate by phosphofructokinase. Interestingly, the rate-limiting glycolytic enzymes (phosphofructokinase, hexokinase, and pyruvate kinase) were not detected to be differentially abundant in the present study.

Previous proteomic research has reported differential abundance of glycolytic enzymes between beef muscles (LL vs. PM; Joseph et al., 2012) and within the same muscle (LL) from different carcasses exhibiting differential color stability (Canto et al., 2015). The glycolytic metabolism can stimulate production of NADH and pyruvate in postmortem skeletal muscles. NADH is an important cofactor in enzymatic and non-enzymatic metmyoglobin reduction, whereas pyruvate is a mitochondrial substrate that promotes NADH regeneration (Ramanathan and

Mancini, 2010). The greater abundance of glycolytic enzymes in muscles with greater color stability (LL and ST) compared to color-labile muscle (PM) in the current study indicated that these muscles have greater capacity to regenerate NADH for subsequent metmyoglobin reduction, thereby stabilizing beef color. Therefore, future research should focus on these differentially abundant glycolytic enzymes to clearly understand their functional roles in postmortem muscles governing meat color.

Proteins related to energy metabolism

Creatine kinase M-type, L-lactate dehydrogenase A, malate dehydrogenase (cytoplasmic and mi-

Table 8. Differentially abundant sarcoplasmic proteins in beef *longissimus lumborum* (LL), *psoas major* (PM), and *semitendinosus* (ST) steaks ($n = 8$) on d 14 of aging

Protein	Accession number	Score/matched peptides	Sequence coverage, %	Over-abundant	Spot ratio	Function
LL14 vs. PM14						
Mitochondrial heat shock protein (60 kDa)	P31081	3120.65/58	79.23	PM14	0.50 ^a	Chaperone
Mitochondrial heat shock protein (60kDa)	P31081	2742.17/54	74.87	PM14	0.42 ^a	Chaperone
Malate dehydrogenase (cytoplasmic)	Q3T145	844.93/30	61.68	LL14	1.71 ^a	Energy metabolism
Beta-enolase	Q3ZC09	1561.88/31	69.12	LL14	1.53 ^a	Glycolytic enzyme
Aldehyde dehydrogenase (mitochondrial)	P20000	1904.42/34	56.35	LL14	1.96 ^a	Energy metabolism
Aldehyde dehydrogenase (mitochondrial)	P20000	3277.11/38	61.15	LL14	1.68 ^a	Energy metabolism
Phosphoglucomutase-1	Q08DP0	2524.35/58	85.23	PM14	0.45 ^a	Glycolytic enzyme
Glycerol-3-phosphate dehydrogenase (cytoplasmic)	Q5EA88	2402.72/31	93.41	LL14	1.57 ^a	Energy metabolism
Creatine kinase M-type	Q9XSC6	1404.39/32	74.54	LL14	1.97 ^a	Energy metabolism
Glycerol-3-phosphate dehydrogenase (cytoplasmic)	Q5EA88	2258.30/28	73.93	LL14	1.75 ^a	Energy metabolism
Glycerol-3-phosphate dehydrogenase (cytoplasmic)	Q5EA88	2402.71/28	82.23	LL14	1.63 ^a	Energy metabolism
Phosphoglucomutase-1	Q08DP0	4184.83/59	84.52	LL14	4.13 ^a	Glycolytic enzyme
Phosphoglucomutase-1	Q08DP0	2750.32/48	74.73	LL14	4.07 ^a	Glycolytic enzyme
Creatine kinase M-type	Q9XSC6	469.23/19	41.21	LL14	2.07 ^a	Energy metabolism
LL14 vs. ST14						
Malate dehydrogenase (cytoplasmic)	Q3T145	1121.78/26	55.99	LL14	1.69 ^b	Energy metabolism
Phosphoglucomutase-1	Q08DP0	2635.82/53	72.42	LL14	1.54 ^b	Glycolytic enzyme
Beta-enolase	Q3ZC09	1975.11/50	74.42	ST14	0.57 ^b	Glycolytic enzyme
Phosphoglucomutase-1	Q08DP0	1166.63/54	68.51	LL14	2.02 ^b	Glycolytic enzyme
Phosphoglucomutase-1	Q08DP0	5453.43/64	84.70	LL14	1.91 ^b	Glycolytic enzyme
Phosphoglucomutase-1	Q08DP0	4422.10/58	72.42	LL14	1.85 ^b	Glycolytic enzyme
PM14 vs. ST14						
Mitochondrial heat shock protein (60kDa)	P31081	2027.34/54	71.03	PM14	1.69 ^c	Chaperone
Mitochondrial heat shock protein (60kDa)	P31081	2623.44/54	76.61	PM14	1.92 ^c	Chaperone
Beta-enolase	Q3ZC09	2335.71/44	66.59	ST14	0.62 ^c	Glycolytic enzyme
Serotransferrin	Q29443	2913.00/70	73.72	PM14	1.82 ^c	Transport protein
Glyceraldehyde-3-phosphate dehydrogenase	P10096	1332.36/25	64.56	ST14	0.65 ^c	Glycolytic enzyme
Creatine kinase M-type	Q9XSC6	4731.45/54	83.20	ST14	0.50 ^c	Energy metabolism

^aSpot ratio of LL14/PM14.^bSpot ratio of LL14/ST14.^cSpot ratio of PM14/ST14.

tochondrial), glycerol-3-phosphate dehydrogenase, alanine aminotransferase 1, aldehyde dehydrogenase (mitochondrial), ATP synthase, and adenylate kinase isoenzyme 1 were the enzymes/proteins related to energy metabolism that were differentially abundant ($P < 0.05$) between the treatment groups. Similar to the glycolytic enzymes, in general, these proteins were more abundant in LL and ST compared to PM through the aging days (Tables 6 to 10). As mentioned earlier, this could be a reflection of the inherent differences in fiber composition of these muscles. There were no metabolic enzymes differentially abundant ($P > 0.05$) between LL and ST on 0 and 7-d aging. The LL14 had more cytoplasmic malate dehydrogenase than ST14 (Table 8), whereas ST21 had more lactate dehydrogenase than LL21 (Table 9). These results indicated that LL and ST

had very similar energy metabolism during the post-mortem period, whereas PM differed significantly.

Metabolic proteins were differentially abundant within muscles during aging ($P < 0.05$; Tables 10 to 12). In general, these proteins (except malate dehydrogenase) were more abundant in aged samples compared to non-aged samples in LL and ST. In PM, creatine kinase M-type was more abundant ($P < 0.05$) in PM0 compared to PM7, whereas mitochondrial ATP synthase was more abundant ($P < 0.05$) in PM14 compared to PM0 (Table 11), which suggested that sarcoplasmic proteome of PM behaves differently than LL and ST during postmortem aging.

Creatine kinase M-type is a metabolic enzyme that plays a critical role in maintaining the ATP-ADP levels during immediate postmortem period by catalyz-

Table 9. Differentially abundant sarcoplasmic proteins in beef *longissimus lumborum* (LL), *psaos major* (PM), and *semitendinosus* (ST) steaks ($n = 8$) on d 21 of aging

Protein	Accession number	Score/matched peptides	Sequence coverage, %	Over-abundant	Spot ratio	Function
LL21 vs. PM21						
Serum albumin	P02769	6940.19/67	83.69	LL21	1.64 ^a	Transport
Serum albumin	P02769	915.42/39	56.05	LL21	1.61 ^a	Transport
Creatine kinase M-type	Q9XSC6	2413.26/52	81.10	LL21	2.33 ^a	Energy metabolism
Triosephosphate isomerase	Q5E956	7139.71/32	93.98	LL21	1.73 ^a	Glycolytic enzyme
Creatine kinase M-type	Q9XSC6	9693.28/57	82.68	LL21	2.43 ^a	Energy metabolism
LL21 vs. ST21						
Heat shock protein (70 kDa)	Q27975	5755.16/64	72.85	LL21	4.06 ^b	Chaperone
L-lactate dehydrogenase A	P19858	1494.08/42	96.08	ST21	0.41 ^b	Energy metabolism
PM21 vs. ST21						
Mitochondrial heat shock protein (60 kDa)	P31081	3178.58/62	76.27	PM21	2.07 ^c	Chaperone
Serum albumin	P02769	10170.79/86	88.47	PM21	1.93 ^c	Transport
Stress-induced-phosphoprotein 1	Q3ZBZ8	2142.54/73	79.19	PM21	1.73 ^c	Chaperone
Creatine kinase M-type	Q9XSC6	1897.54/49	71.65	ST21	0.47 ^c	Energy metabolism
Creatine kinase M-type	Q9XSC6	2550.50/51	78.22	ST21	0.54 ^c	Energy metabolism
Triosephosphate isomerase	Q5E956	7214.08/30	93.98	ST21	0.50 ^c	Glycolytic enzyme
Creatine kinase M-type	Q9XSC6	5657.84/56	81.10	ST21	0.45 ^c	Energy metabolism
Glyceraldehyde-3-phosphate dehydrogenase	P10096	532.90/17	54.35	ST21	0.28 ^c	Glycolytic enzyme
Creatine kinase M-type	Q9XSC6	7145.41/64	83.73	ST21	0.55 ^c	Energy metabolism
Malate dehydrogenase (mitochondrial)	Q32LG3	4349.40/37	75.74	ST21	0.65 ^c	Energy metabolism

^aSpot ratio of LL21/PM21.^bSpot ratio of LL21/ST21.^cSpot ratio of PM21/ST21.**Table 10.** Differentially abundant sarcoplasmic proteins during aging (0, 7, 14, and 21 d) in beef *longissimus lumborum* (LL) steaks ($n = 8$)

Protein	Accession number	Score/matched peptides	Sequence coverage, %	Over-abundant	Spot ratio	Function
LL0 vs. LL7						
Adenylate kinase isoenzyme 1	P00570	2973.04/45	92.78	LL7	0.43 ^a	Energy metabolism
Myoglobin	P02192	2485.84/20	93.51	LL7	0.33 ^a	Oxygen transport
LL0 vs. LL14						
Heat shock cognate protein (71 kDa)	P19120	4076.93/56	74.31	LL14	0.41 ^b	Chaperone
Beta-enolase	Q3ZC09	2611.05/47	71.66	LL14	0.58 ^b	Glycolytic enzyme
Alanine aminotransferase 1	A4IFH5	361.85/18	44.35	LL14	0.59 ^b	Energy metabolism
Phosphoglucosmutase-1	Q08DP0	1946.54/49	77.05	LL14	0.52 ^b	Glycolytic enzyme
Creatine kinase M-type	Q9XSC6	405.71/16	37.27	LL14	0.64 ^b	Energy metabolism
Phosphoglucosmutase-1	Q08DP0	1290.88/46	69.75	LL14	0.53 ^b	Glycolytic enzyme
Beta-enolase	Q3ZC09	7628.55/61	84.79	LL14	0.60 ^b	Glycolytic enzyme
LL0 vs. LL21						
Alpha-enolase	Q9XSJ4	778.37/28	61.75	LL21	0.42 ^c	Glycolytic enzyme
Malate dehydrogenase (cytoplasmic)	Q3T145	1746.38/36	61.68	LL0	1.89 ^c	Energy metabolism
Alpha-enolase	Q9XSJ4	1142.73/32	66.59	LL21	0.66 ^c	Glycolytic enzyme
Alpha-enolase	Q9XSJ4	3031.52/41	69.59	LL21	0.60 ^c	Glycolytic enzyme
Glyceraldehyde-3-phosphate dehydrogenase	P10096	1727.91/26	69.67	LL0	2.90 ^c	Glycolytic enzyme

^aSpot ratio of LL0/LL7.^bSpot ratio of LL0/LL14.^cSpot ratio of LL0/LL21.

ing the interconversion of ADP and phosphocreatine to generate ATP and creatine. In postmortem muscles, depletion of ATP due to anoxia leads to the utilization of phosphocreatine to produce ATP and creatine. Previous studies have indicated that creatine can also act as an antioxidant by scavenging the free radicals (Sestili et al., 2011; Lawler et al., 2002). Creatine kinase M-type was more abundant ($P < 0.05$) in LL and ST, and these muscles had better color stability compared to PM. In agreement, previous research indicated that fast-twitch muscles with higher activity of glycolytic enzymes have greater creatine kinase content than the oxidative muscles (Okumura et al., 2005). Moreover, previous proteomic investigations have reported a greater abundance of creatine kinase M-type in color-stable muscles compared to color-labile beef muscles (Nair et al., 2016; Canto et al., 2015; Joseph et al., 2012)

Cytoplasmic malate dehydrogenase was more abundant ($P < 0.05$) in LL14 compared to PM14 and ST14 (Table 8), and in LL0 when compared to LL21 (Table 10). Mitochondrial malate dehydrogenase was of greater abundance ($P < 0.05$) in ST21 compared to PM21 (Table 9). Cytoplasmic malate dehydrogenase is responsible for shuttling NADH across the mitochon-

drial membrane via the malate-aspartate shuttle, whereas mitochondrial malate dehydrogenase is a principal enzyme of the citric acid cycle (operated within mitochondria) which catalyzes the conversion of oxaloacetate and malate utilizing the NAD/NADH coenzyme system (Minarik et al., 2002). Mohan et al. (2010a, 2010b) reported that malate decreases metmyoglobin formation in beef muscle homogenates by generating NADH utilizing the malate dehydrogenase enzyme system, which is subsequently used for metmyoglobin reduction. The differential abundance of these enzymes indicates that different muscles could differ in their response to malate enhancement.

Glycerol-3-phosphate dehydrogenase was more abundant ($P < 0.05$) in LL14 compared to PM14 (Table 8). This enzyme is integral to the conversion of triglyceride-derived glycerol into glyceraldehyde-3-phosphate, which then enters the glycolytic pathway. This process can generate NADH, which in turn is utilized for metmyoglobin reduction. Alanine aminotransferase 1 found in greater abundance ($P < 0.05$) in LL14 during aging (Table 10) is a cytoplasmic enzyme catalyzing the reversible transamination between alanine and 2-oxoglutarate to form pyruvate and glutamate. This

Table 11. Differentially abundant sarcoplasmic proteins during aging (0, 7, 14, and 21 d) in beef *psaos major* (PM) steaks ($n = 8$)

Protein	Accession number	Score/matched peptides	Sequence coverage, %	Over-abundant	Spot ratio	Function
PM0 vs. PM7						
Superoxide dismutase [Cu-Zn]	P00442	709.01/11	51.97	PM7	0.59 ^a	Antioxidant
Beta-enolase	Q3ZC09	2075.70/30	65.44	PM7	0.66 ^a	Glycolytic enzyme
Creatine kinase M-type	Q9XSC6	2229.27/48	72.44	PM0	3.43 ^a	Energy metabolism
Beta-enolase	Q3ZC09	4879.07/52	73.73	PM0	2.15 ^a	Glycolytic enzyme
Serotransferrin	Q29443	3879.25/76	74.01	PM0	2.01 ^a	Transport protein
Creatine kinase M-type	Q9XSC6	2784.86/54	74.54	PM0	2.92 ^a	Energy metabolism
Creatine kinase M-type	Q9XSC6	4590.61/58	80.58	PM0	17.86 ^a	Energy metabolism
Myoglobin	P02192	4027.12/29	99.35	PM7	0.66 ^a	Oxygen transport
PM0 vs. PM14						
ATP synthase (beta subunit, mitochondrial)	P00829	2246.52/29	66.29	PM14	0.64 ^b	Energy metabolism
Mitochondrial heat shock protein (60 kDa)	P31081	3370.29/62	72.43	PM14	0.45 ^b	Chaperone
Glyceraldehyde-3-phosphate dehydrogenase	P10096	2311.05/24	61.26	PM0	1.72 ^b	Glycolytic enzyme
Glyceraldehyde-3-phosphate dehydrogenase	P10096	2147.47/25	70.87	PM0	2.27 ^b	Glycolytic enzyme
Glyceraldehyde-3-phosphate dehydrogenase	P10096	2711.18/30	75.98	PM0	1.67 ^b	Glycolytic enzyme
Beta-enolase	Q3ZC09	3993.35/48	76.73	PM14	0.45 ^b	Glycolytic enzyme
PM0 vs. PM21						
Serum albumin	P02769	2090.94/55	78.75	PM0	2.69 ^c	Transport
Glyceraldehyde-3-phosphate dehydrogenase	P10096	1550.64/26	66.37	PM0	8.85 ^c	Glycolytic enzyme
Glyceraldehyde-3-phosphate dehydrogenase	P10096	8266.24/34	84.38	PM0	3.83 ^c	Glycolytic enzyme

^aSpot ratio of PM0/PM7.

^bSpot ratio of PM0/PM14.

^cSpot ratio of PM0/PM21.

enzyme is generally associated with liver health, and its role in meat quality is yet to be clearly understood.

L-Lactate dehydrogenase A was more abundant ($P < 0.05$) in PM0 when compared with ST0 (Table 6), and in ST21 when compared with LL21 (Table 9). During aging, ST21 had greater ($P < 0.05$) lactate dehydrogenase compared to ST0 (Table 12). L-Lactate dehydrogenase catalyzes the inter-conversion of L-lactate and pyruvate with concomitant inter-conversion of NAD^+ and NADH. Kim et al. (2006) reported that lactate enhancement promotes color stability of beef LL through increased lactate dehydrogenase activity and suggested that NADH could be utilized to reduce metmyoglobin. Further, Ramanathan et al. (2010) also reported that NADH generated by lactate dehydrogenase can be used for metmyoglobin reduction through electron-transport-mediated pathways and reductase mediated pathways. The results of the aforementioned studies (Kim et al., 2006; Ramanathan et al., 2010) suggested that the muscles with a greater abundance of lactate dehydrogenase could be better responsive to lactate enhancement for stabilizing meat color. Differential abundance of lactate dehydrogenase observed in the present study indicated

that lactate-enhancement may be employed as a muscle- and aging-specific strategy for color stabilization.

Aldehyde dehydrogenase (mitochondrial; ALDH2) is an enzyme located in the mitochondrial matrix catalyzing the oxidation of acetaldehyde (produced from ethanol) into acetate in a reaction coupled with NAD^+ reduction (Jelski and Szmikowski, 2008). It was detected in greater abundance ($P < 0.05$) in LL14 compared to PM14 (Table 8). ATP synthase was identified to be more abundant ($P < 0.05$) in PM14 when compared to PM0 (Table 11). This enzyme catalyzes ATP synthesis in mitochondria using ADP and phosphate driven by the electron transport chain. The presence of these mitochondrial proteins in the sarcoplasmic proteome could be indicative of the muscle-specific degradation of mitochondria during postmortem aging. Adenylate kinase isoenzyme 1 catalyzes the reversible conversion of ADP to ATP (Heil et al., 1974). This enzyme was more abundant ($P < 0.05$) in LL7 and ST7 compared to LL0 and ST0 respectively (Table 10 and 12), and the 7-d aged steaks had greater surface redness than non-aged steaks (Table 2). In contrast, Canto et al. (2015) reported greater abundance of the adenylate kinase isoenzyme 1 in color-labile LL muscles compared to

Table 12. Differentially abundant sarcoplasmic proteins during aging (0, 7, 14, and 21 d) in *beef semitendinosus* (ST) steaks ($n = 8$)

Protein	Accession number	Score/matched peptides	Sequence coverage, %	Over-abundant	Spot ratio	Function
ST0 vs. ST7						
Protein deglycase DJ-1	Q5E946	814.38/31	97.88	ST7	0.63 ^a	Chaperone
Aldose reductase	P16116	1315.72/27	87.30	ST0	2.11 ^a	Oxidoreductase enzyme
Alpha-enolase	Q9XSJ4	1902.61/37	63.82	ST0	1.83 ^a	Glycolytic enzyme
Myoglobin	P02192	543.18/18	88.96	ST7	0.65 ^a	Oxygen transport
Glyceraldehyde-3-phosphate dehydrogenase	P10096	1866.66/26	65.77	ST0	1.82 ^a	Glycolytic enzyme
Creatine kinase M-type	Q9XSC6	761.7/28	61.68	ST7	0.52 ^a	Energy metabolism
Alpha-crystallin B	P02510	1951.07/27	74.29	ST0	1.97 ^a	Chaperone
Polyubiquitin-C	P0CH28	517.25/16	93.91	ST7	0.37 ^a	Ubiquitylation
Beta-enolase	Q3ZC09	6352.87/47	72.12	ST7	0.44 ^a	Glycolytic enzyme
Adenylate kinase isoenzyme 1	P00570	2504.89/27	84.54	ST7	0.57 ^a	Adenosine phosphate metabolism
ST0 vs. ST14						
Beta-enolase	Q3ZC09	2385.59/51	74.65	ST14	0.39 ^b	Glycolytic enzyme
Beta-enolase	Q3ZC09	3827.11/54	76.04	ST14	0.55 ^b	Glycolytic enzyme
Beta-enolase	Q3ZC09	2811.22/53	76.50	ST14	0.36 ^b	Glycolytic enzyme
Beta-enolase	Q3ZC09	4151.38/56	83.41	ST14	0.53 ^b	Glycolytic enzyme
Beta-enolase	Q3ZC09	3431.61/62	83.87	ST14	0.29 ^b	Glycolytic enzyme
ST0 vs. ST21						
Serum albumin	P02769	2513.53/61	81.05	ST21	0.48 ^c	Transport
Serum albumin	P02769	1952.95/61	81.38	ST0	2.05 ^c	Transport
L-lactate dehydrogenase A	P19858	1662.30/35	92.77	ST21	0.64 ^c	Energy metabolism

^aSpot ratio of ST0/ST7.

^bSpot ratio of ST0/ST14.

^cSpot ratio of ST0/ST21.

color-stable LL counterparts aged for 13 d. This observed variation could be a result of the difference in aging days. However, the exact mechanism through which this enzyme influences meat color is not clearly understood.

Antioxidant proteins

Superoxide dismutase scavenges superoxide anions by forming hydrogen peroxide (Aebi 1974; Mercier et al., 2004). Two types of superoxide dismutase were identified as differentially abundant between the treatment groups. Mitochondrial superoxide dismutase [Mn] (SOD2) was more abundant ($P < 0.05$) in PM0 compared to ST0 (Table 6). SOD2 is generally located in the mitochondrial matrix, and its presence in sarcoplasm could be a result of the protein's disassociation from mitochondria in postmortem muscles. The greater abundance of SOD2 in PM0 than in ST0 suggests that the integrity of mitochondria in PM and ST early postmortem are different and that this protein could be utilized as a potential indicator of mitochondrial damage. Superoxide dismutase [Cu-Zn] (SOD1) was detected in greater abundance ($P < 0.05$) in PM7 compared to ST7 and PM0 (Tables 7 and 11). In postmortem muscles, superoxide dismutase acts in conjunction with catalase to limit lipid oxidation. The catalase enzymes reduce hydrogen peroxide formed by superoxide dismutase to water and oxygen (Aebi, 1974). However, in the present study, catalase was not detected among the differentially abundant proteins. In general, oxidative muscles (such as PM) have greater activities of superoxide dismutase and catalase than glycolytic muscles (Terevinto et al., 2010). Renerre et al. (1996) reported that the increase in the activities of the antioxidant enzymes of color-labile muscles such as PM and diaphragm could be a defensive mechanism to the increased oxidative stress in such muscles during postmortem.

Chaperones

Heat shock cognate protein (71 kDa), heat shock protein (70 kDa), mitochondrial heat shock protein (60 kDa), stress-induced-phosphoprotein 1, α -crystallin B, and protein deglycase DJ-1 were the chaperone proteins identified to be differentially abundant ($P < 0.05$). Heat shock cognate protein (71 kDa) is a repressor of transcriptional activation and can act as a molecular chaperone. It was more abundant ($P < 0.05$) in LL7 (in comparison with PM7 and ST7; Table 7) and in LL14 (in comparison with LL0; Table 10). However, heat shock protein (70 kDa) was more abundant ($P < 0.05$) in LL21 than in ST21 (Table 9). This protein prevents protein aggregation in cytosol in combination with

other chaperones. Mitochondrial heat shock protein (60 kDa) is responsible for the correct folding of imported proteins to the mitochondrial matrix. In general, it was detected in increased abundance in aged PM samples (in PM14 compared to LL14, ST14, and PM0; in PM21 compared to ST21; Tables 8, 9, and 11), indicating a greater mitochondrial damage in PM during aging.

Stress induced-phosphoprotein 1, which was more abundant ($P < 0.05$) in PM21 compared to ST21 (Table 9), functions as a co-chaperone by linking and modulating heat shock protein 70 and heat shock protein 90 (Ogunuga et al., 2004). Alpha-crystallin B has chaperone-like activity, preventing aggregation of various proteins under stress conditions. This protein was more abundant ($P < 0.05$) in ST0 compared to ST7 (Table 12). Protein deglycase DJ-1 protects cells against oxidative stress and cell death by acting as an oxidative stress sensor, redox-sensitive chaperone, and protease. The protein was more abundant in ST7 compared to ST0 (Table 12), and has been previously identified to be differentially abundant in sarcoplasmic proteome in relation to meat color (Joseph et al., 2012; Wu et al., 2016), tenderness (Jia et al., 2009), and water holding capacity (Hwang et al., 2005). In general, chaperone proteins can prevent protein aggregation and protein denaturation occurring during the muscle-to-meat conversion (Sayd et al., 2006). Previous research by Joseph et al. (2012) reported that stress-induced phosphoprotein 1 was positively correlated to color stability in beef LL steaks.

Transport proteins

Myoglobin, serum albumin, and serotransferrin were the transport proteins differentially abundant between the treatments. Biochemical analyses using spectrophotometry also indicated variations in myoglobin concentration among the beef muscles ($P < 0.0001$); PM had the greatest myoglobin concentration (5.54 mg/g), followed by LL (4.35 mg/g), and ST (4.05 mg/g). Sarcoplasmic proteome profiling also confirmed this muscle-specificity in myoglobin concentration. The PM on 0-d and 7-d aging had greater ($P < 0.05$) abundance of myoglobin in the sarcoplasmic proteome than LL and ST on the same days (Table 6 and 7). However, sarcoplasmic proteome analysis did not detect a difference in myoglobin concentration among the muscles on 14-d and 21-d aging. Myoglobin abundance in the sarcoplasmic proteome was also influenced by aging, with LL7, PM7, and ST7 having greater ($P < 0.05$) abundance of myoglobin compared to their 0-d aged counterparts (Tables 10 to 12). This observation coincides with the greatest red-

ness observed in steaks after 7-d aging (Table 2). The differential abundance of myoglobin in sarcoplasmic proteome observed in the current study could be either due to a difference in the total concentration of myoglobin or due to post-translational modification of the heme protein. Previous studies have reported that myoglobin isoforms (potentially due to protein phosphorylation) vary between color-stable and color-labile LL muscles (Canto et al., 2015). Further research would be valuable in understanding the relationship between myoglobin phosphorylation and beef color stability.

Serum albumin can function as a transport protein and antioxidant protein, although its main function is the regulation of the colloidal osmotic pressure of blood (Roche et al., 2008). There was no definite pattern in the differential abundance of this protein. Serotransferrin is an iron binding transport protein and was found in lower abundance in ST0 compared to LL0 and PM0 (Table 6). Joseph et al. (2012) reported greater abundance of this protein in color-labile PM. However, the potential role of these 2 proteins in meat quality is yet to be clearly understood.

Conclusions

The present study provided a comprehensive evaluation of color traits and sarcoplasmic proteome profile of 3 beef muscles (LL, PM, and ST) with differential color stability during postmortem aging. Muscle source and aging influenced the color attributes and sarcoplasmic proteome. The color stability followed the order: LL > ST > PM, and the 7-d aged steaks demonstrated the greatest surface redness. Glycolytic enzymes, proteins associated with energy metabolism, antioxidant proteins, chaperones, and transport proteins were differentially abundant between the muscles and aging time points. Overall, glycolytic enzymes were of greater abundance in muscles and at aging times with increased color stability and redness. The differential abundance of sarcoplasmic proteome components indicates that these intrinsic factors play a critical role in color stability of postmortem beef muscles. Additionally, these results provide potential protein biomarkers to be focused in future research on muscle-specific beef color stability during postmortem aging.

Literature Cited

- Aebi, H. 1974. Catalase. In: H. U. Bergmeyer, editor, *Methods of enzymatic analysis*. Academic Press, New York. p. 673–684, doi:10.1016/B978-0-12-091302-2.50032-3.
- Albery, W. J., and J. R. Knowles. 1976. Free-energy profile for the reaction catalyzed by triosephosphate isomerase. *Biochemistry* 15:5627–5631. doi:10.1021/bi00670a031
- American Meat Science Association. 2012. *Meat color measurement guidelines*. 2nd ed. Am. Meat Sci. Assoc., Chicago, IL.
- Anderson, M. J., S. M. Lonergan, and E. Huff-Lonergan. 2014. Differences in phosphorylation of phosphoglucosylase 1 in beef steaks from the longissimus dorsi with high or low star probe values. *Meat Sci.* 96:379–384. doi:10.1016/j.meatsci.2013.07.017
- Belskie, K. M., R. Ramanathan, S. P. Suman, and R. A. Mancini. 2015. Effects of muscle type and display time on beef mitochondria. *Meat Sci.* 157–158. doi:10.1016/j.meatsci.2014.09.132
- Bradford, M. M. 1976. A rapid and sensitive method for the quantitation of microgram quantities of protein utilizing the principle of protein-dye binding. *Anal. Biochem.* 72:248–254. doi:10.1016/0003-2697(76)90527-3
- Canto, A. C. V. C. S., S. P. Suman, M. N. Nair, S. Li, G. Rentfrow, C. M. Beach, T. J. P. Silva, T. L. Wheeler, S. D. Shackelford, A. Grayson, R. O. McKeith, and D. A. King. 2015. Differential abundance of sarcoplasmic proteome explains animal effect on beef longissimus lumborum color stability. *Meat Sci.* 102:90–98. doi:10.1016/j.meatsci.2014.11.011
- Canto, A. C. V. C. S., B. R. C. Costa-Lima, S. P. Suman, M. L. G. Monteiro, F. M. Viana, A. P. A. A. Salim, M. N. Nair, T. J. Silva, and C. A. Conte-Junior. 2016. Color attributes and oxidative stability of longissimus lumborum and psoas major muscles from Nellore bulls. *Meat Sci.* 121:19–26. doi:10.1016/j.meatsci.2016.05.015
- Clerens, S., A. Thomas, J. Gathercole, J. E. Plowman, T. Y. Yu, A. J. Grosvenor, S. R. Haines, P. Dobbie, K. Taukiri, K. Rosenvold, J. M. Dyer, and S. Deb-Choudhury. 2016. Proteomic and peptidomic differences and similarities between four muscle types from New Zealand raised Angus steers. *Meat Sci.* 121:53–63. doi:10.1016/j.meatsci.2016.05.014
- Cori, G. T., S. P. Colowick, and C. F. Cori. 1938. The formation of glucose-1-phosphoric acid in extracts of mammalian tissues and of yeast. *J. Biol. Chem.* 123:375–380.
- English, A. R., G. G. Mafi, D. L. VanOverbeke, and R. Ramanathan. 2016. Effects of extended aging and modified atmospheric packaging on beef top loin steak color. *J. Anim. Sci.* 94:1727–1737. doi:10.2527/jas.2015-0149
- Faustman, C., Q. Sun, R. Mancini, and S. P. Suman. 2010. Myoglobin and lipid oxidation interactions: Mechanistic bases and control. *Meat Sci.* 86:86–94. doi:10.1016/j.meatsci.2010.04.025
- Guelker, M., A. N. Haneklaus, J. C. Brooks, C. C. Carr, R. J. Delmore, D. B. Griffin, D. S. Hale, K. B. Harris, G. G. Mafi, D. D. Johnson, C. L. Lorenzen, R. J. Maddock, J. N. Martin, R. K. Miller, C. R. Raines, D. L. VanOverbeke, L. L. Vedral, B. E. Wasser, and J. W. Savell. 2013. National Beef Tenderness Survey–2010: Warner-Bratzler shear force values and sensory panel ratings for beef steaks from United States retail and food service establishments. *J. Anim. Sci.* 91:1005–1014. doi:10.2527/jas.2012-5785
- Heil, A., G. Muller, L. Noda, T. Pinder, H. Schirmer, I. Schirmer, and I. Von Zabern. 1974. The amino-acid sequence of porcine adenylate kinase from skeletal muscle. *FEBS J.* 43:131–144. doi:10.1111/j.1432-1033.1974.tb03393.x
- Hoorn, R. K. J., J. P. Flikweert, and G. E. J. Staal. 1974. Purification and properties of enolase of human erythrocytes. *Int. J. Biochem.* 5:845–852. doi:10.1016/0020-711X(74)90119-0
- Hunt, M. C., and H. B. Hedrick. 1977. Profile of fiber types and related properties of five bovine muscles. *J. Food Sci.* 42:513–517. doi:10.1111/j.1365-2621.1977.tb01535.x

- Hwang, I. H., B. Y. Park, J. H. Kim, S. H. Cho, and J. M. Lee. 2005. Assessment of postmortem proteolysis by gel-based proteome analysis and its relationship to meat quality traits in pig longissimus. *Meat Sci.* 69:79–91. doi:10.1016/j.meatsci.2004.06.019
- Jelski, W., and M. Szmitkowski. 2008. Alcohol dehydrogenase (ADH) and aldehyde dehydrogenase (ALDH) in the cancer diseases. *Clin. Chim. Acta* 395:1–5. doi:10.1016/j.cca.2008.05.001
- Jia, X., E. Veiseth-Kent, H. Grove, P. Kuziora, L. Aass, K. I. Hildrum, and K. Hollung. 2009. Peroxiredoxin-6-a potential protein marker for meat tenderness in bovine longissimus thoracis muscle. *J. Anim. Sci.* 87:2391–2399. doi:10.2527/jas.2009-1792
- Joseph, P., S. P. Suman, G. Rentfrow, S. Li, and C. M. Beach. 2012. Proteomics of muscle-specific beef color stability. *J. Agric. Food Chem.* 60:3196–3203. doi:10.1021/jf204188v
- Kim, J. W., and C. V. Dang. 2005. Multifaceted roles of glycolytic enzymes. *Trends Biochem. Sci.* 30:142–150. doi:10.1016/j.tibs.2005.01.005
- Kim, Y. H., M. C. Hunt, R. A. Mancini, M. Seyfert, T. M. Loughin, D. H. Kropf, and J. S. Smith. 2006. Mechanism for lactate-color stabilization in injection-enhanced beef. *J. Agric. Food Chem.* 54:7856–7862. doi:10.1021/jf061225h
- King, D. A., S. D. Shackelford, N. Kalchayanand, and T. L. Wheeler. 2012. Sampling and aging effects on beef longissimus color stability measurements. *J. Anim. Sci.* 90:3596–3605. doi:10.2527/jas.2011-4871
- Kirchofer, K. S., C. B. Calkins, and B. L. Gwartney. 2002. Fiber-type composition of muscles of the beef chuck and round. *J. Anim. Sci.* 80:2872–2878. doi:10.2527/2002.80112872x
- Lawler, J. M., W. S. Barnes, G. Wu, W. Song, and S. Demaree. 2002. Direct antioxidant properties of creatine. *Biochem. Biophys. Res. Commun.* 290:47–52. doi:10.1006/bbrc.2001.6164
- Lee, M. S., J. K. Apple, J. W. Yancey, J. T. Sawyer, and Z. B. Johnson. 2008. Influence of vacuum-aging period on bloom development of the beef gluteus medius from top sirloin butts. *Meat Sci.* 80:592–598. doi:10.1016/j.meatsci.2008.02.006
- MacDougall, D. B. 1982. Changes in the colour and opacity of meat. *Food Chem.* 9:75–88. doi:10.1016/0308-8146(82)90070-X
- Mancini, R. A., and M. C. Hunt. 2005. Current research in meat color. *Meat Sci.* 71:100–121. doi:10.1016/j.meatsci.2005.03.003
- Mancini, R. A., and R. Ramanathan. 2014. Effects of postmortem storage time on color and mitochondria in beef. *Meat Sci.* 98:65–70. doi:10.1016/j.meatsci.2014.04.007
- Mancini, R. A., S. P. Suman, M. K. R. Konda, and R. Ramanathan. 2009. Effect of carbon monoxide packaging and lactate-enhancement on the color stability of beef steaks stored at 1°C for 9 days. *Meat Sci.* 81:71–76. doi:10.1016/j.meatsci.2008.06.021
- Marino, R., M. Albenzio, A. della Malva, M. Caroprese, A. Santillo, and A. Sevi. 2014. Changes in meat quality traits and sarcoplasmic proteins during aging in three different cattle breeds. *Meat Sci.* 98:178–186. doi:10.1016/j.meatsci.2014.05.024
- McKenna, D. R., P. D. Mies, B. E. Baird, K. D. Pfeiffer, J. W. Ellebracht, and J. W. Savell. 2005. Biochemical and physical factors affecting discoloration characteristics of 19 bovine muscles. *Meat Sci.* 70:665–682. doi:10.1016/j.meatsci.2005.02.016
- Mercier, Y., P. Gatellier, and M. Renner. 2004. Lipid and protein oxidation in vitro, and antioxidant potential in meat from Charolais cows finished on pasture or mixed diet. *Meat Sci.* 66:467–473. doi:10.1016/S0309-1740(03)00135-9
- Minarik, P., N. Tomaskova, M. Kollarova, and M. Antalik. 2002. Malate dehydrogenases-structure and function. *Gen. Physiol. Biophys.* 21:257–266.
- Mohan, A., M. C. Hunt, T. J. Barstow, T. A. Houser, and S. Muthukrishnan. 2010a. Effects of malate, lactate, and pyruvate on myoglobin redox stability in homogenates of three bovine muscles. *Meat Sci.* 86:304–310. doi:10.1016/j.meatsci.2010.04.030
- Mohan, A., M. C. Hunt, S. Muthukrishnan, T. J. Barstow, and T. A. Houser. 2010b. Myoglobin redox form stabilization by compartmentalized lactate and malate dehydrogenases. *J. Agric. Food Chem.* 58:7021–7029. doi:10.1021/jf100714g
- Nair, M. N., S. P. Suman, M. K. Chatli, S. Li, P. Joseph, C. M. Beach, and G. Rentfrow. 2016. Proteome basis for intramuscular variation in color stability of beef semimembranosus. *Meat Sci.* 113:9–16. doi:10.1016/j.meatsci.2015.11.003
- Neethling, N. E., S. P. Suman, G. O. Sigge, L. C. Hoffman, and M. C. Hunt. 2017. Exogenous and endogenous factors influencing color of fresh meat from ungulates. *Meat Muscle Biol.* 1:253–275. doi:10.22175/mmb2017.06.0032
- Odunuga, O. O., V. M. Longshaw, and G. L. Blatch. 2004. Hop:more than an Hsp70/Hsp90 adaptor protein. *BioEssays* 26:1058–1068. doi:10.1002/bies.20107
- Okumura, N., A. Hashida-Okumura, K. Kita, M. Matsubae, T. Matsubara, T. Takao, and K. Nagai. 2005. Proteomic analysis of slow-and fast-twitch skeletal muscles. *Proteomics* 5:2896–2906. doi:10.1002/pmic.200401181
- Ramanathan, R., and R. A. Mancini. 2010. Effects of pyruvate on bovine heart mitochondria-mediated metmyoglobin reduction. *Meat Sci.* 86:738–741. doi:10.1016/j.meatsci.2010.06.014
- Ramanathan, R., R. A. Mancini, and N. B. Maheswarappa. 2010. Effects of lactate on bovine heart mitochondria-mediated metmyoglobin reduction. *J. Agric. Food Chem.* 58:5724–5729. doi:10.1021/jf1002842
- Renner, M., F. Dumont, and P. Gatellier. 1996. Antioxidant enzyme activities in beef in relation to oxidation of lipid and myoglobin. *Meat Sci.* 43:111–121. doi:10.1016/0309-1740(96)84583-9
- Roche, M., P. Rondeau, N. R. Singh, E. Tarnus, and E. Bourdon. 2008. The antioxidant properties of serum albumin. *FEBS Lett.* 582:1783–1787. doi:10.1016/j.febslet.2008.04.057
- Sammel, L. M., M. C. Hunt, D. H. Kropf, K. A. Hachmeister, and D. E. Johnson. 2002. Comparison of assays for metmyoglobin reducing ability in beef inside and outside semimembranosus muscle. *J. Food Sci.* 67:978–984. doi:10.1111/j.1365-2621.2002.tb09439.x
- Sayd, T., M. Morzel, C. Chambon, M. Franck, P. Figwer, C. Larzul, P. Le Roy, G. Monin, P. Cherel, and E. Laville. 2006. Proteome analysis of the sarcoplasmic fraction of pig semimembranosus muscle:implications on meat color development. *J. Agric. Food Chem.* 54:2732–2737. doi:10.1021/jf052569v
- Sestili, P., C. Martinelli, E. Colombo, E. Barbieri, L. Potenza, S. Sartini, and C. Fimognari. 2011. Creatine as an antioxidant. *Amino Acids* 40:1385–1396. doi:10.1007/s00726-011-0875-5

- Seyfert, M., R. A. Mancini, M. C. Hunt, J. Tang, C. Faustman, and M. Garcia. 2006. Color stability, reducing activity, and cytochrome c oxidase activity of five bovine muscles. *J. Agric. Food Chem.* 54:8919–8925. doi:10.1021/jf061657s
- Smith, G. C., K. E. Belk, J. N. Sofos, J. D. Tatum, and S. N. Williams. 2000. Economic implications of improved color stability in beef. In: E. A. Decker, C. Faustman, and C. J. Lopez-Bote, editors, *Antioxidants in muscle foods: Nutritional strategies to improve quality*. Wiley Intersci, New York. p. 397–426.
- Suman, S. P., and P. Joseph. 2013. Myoglobin chemistry and meat color. *Annu. Rev. Food Sci. Technol.* 4:79–99. doi:10.1146/annurev-food-030212-182623
- Suman, S. P., M. C. Hunt, M. N. Nair, and G. Rentfrow. 2014. Improving beef color stability: Practical strategies and underlying mechanisms. *Meat Sci.* 98:490–504. doi:10.1016/j.meatsci.2014.06.032
- Suman, S. P., and M. N. Nair. 2017. Current developments in fundamental and applied aspects of meat color. In: P. P. Purslow, editor, *New Aspects of Meat Quality: From Genes to Ethics*. chap 6. Elsevier, Oxford, United Kingdom. p. 111–127, doi:10.1016/B978-0-08-100593-4.00007-2.
- Terevinto, A., A. Ramos, G. Castroman, M. C. Cabrera, and A. Saadoun. 2010. Oxidative status, in vitro iron-induced lipid oxidation and superoxide dismutase, catalase and glutathione peroxidase activities in rhea meat. *Meat Sci.* 84:706–710. doi:10.1016/j.meatsci.2009.11.007
- Von Seggern, D. D., C. R. Calkins, D. D. Johnson, J. E. Brickler, and B. L. Gwartney. 2005. Muscle profiling: Characterizing the muscles of the beef chuck and round. *Meat Sci.* 71:39–51. doi:10.1016/j.meatsci.2005.04.010
- Wu, W., X. G. Gao, Y. Dai, Y. Fu, X. M. Li, and R. T. Dai. 2015. Post-mortem changes in sarcoplasmic proteome and its relationship to meat color traits in *M. semitendinosus* of Chinese Luxi yellow cattle. *Food Res. Int.* 72:98–105. doi:10.1016/j.foodres.2015.03.030
- Wu, W., Q. Q. Yu, Y. Fu, X. J. Tian, F. Jia, X. M. Li, and R. T. Dai. 2016. Towards muscle-specific meat color stability of Chinese Luxi yellow cattle: A proteomic insight into post-mortem storage. *J. Proteomics* 147:108–118. doi:10.1016/j.jprot.2015.10.027